# Highly catalytic activity of Mn/SBA-15 catalysts for toluene combustion improved by adjusting the morphology of supports

Yuan Qin, Zhenping Qu*, Cui Dong, Yan Wang, Na Huang

*Key Laboratory of Industrial Ecology and Environmental Engineering (MOE), School of Environmental Science and Technology, Dalian University of Technology, Dalian 116024, China*

## ARTICLE INFO

## ABSTRACT

Rod-like, hexagonal and fiber-like SBA-15 mesoporous silicas were synthesized to support $MnO_x$ for toluene oxidation. This study showed that the morphology of the supports greatly influenced the catalytic activity in toluene oxidation. $MnO_x$ supported on rod-like SBA-15 (R-SBA-15) displayed the best catalytic activity and the conversion at 230°C reached more than 90%, which was higher than the other two catalysts. $MnO_x$ species consisted of coexisting $MnO_2$ and $Mn_2O_3$ on the three kinds of SBA-15 samples. Large amounts of $Mn_2O_3$ species were formed on the surface and high oxygen mobility was obtained on $MnO_x$ supported on R-SBA-15, according to the $H_2$ temperature programmed reduction ($H_2$-TPR) and X-ray photoelectron spectroscopy (XPS) results. The Mn/R-SBA-15 catalyst with greater amounts of $Mn_2O_3$ species possessed a large amount of surface lattice oxygen, which accelerated the catalytic reaction rate. Therefore, the surface lattice oxygen and high oxygen mobility were critical factors on the catalytic activity of the Mn/R-SBA-15 catalyst.

© 2018 The Research Center for Eco-Environmental Sciences, Chinese Academy of Sciences. Published by Elsevier B.V.

## Introduction

Volatile organic compounds (VOCs) not only contribute to air pollution, but also cause harm to human health. Therefore, quite a lot of research on VOC elimination has been conducted all over the world. Of the measures used, catalytic oxidation is an effective method to transform VOCs to $CO_2$ and $H_2O$ completely over catalysts at relatively low temperatures. Noble metals, such as Pd, Pt, Au and Ag (Guo et al., 2017; He et al., 2012; Yang et al., 2016), are widely applied for VOC catalytic oxidation, but the most serious challenges for noble metal catalysts are high cost and instability. As a result, the development of non-noble catalysts with low cost is a major issue needing urgent solution.

Transition metal oxides have attracted researchers' interest due to their low cost and good catalytic activity as well as stability. In general, transition metals possess a variety of valence states, so redox reaction takes place together with the transformation of valence states, and this transformation can be the key factor in their catalytic activity. Among the transition metals, manganese oxides have especially high oxygen storage/release capacities and exhibit high activity in catalytic reactions; thus, they are widely applied in the elimination of VOCs, CO and other hazardous gases (Du et al., 2018; Liao et al., 2014; Lu et al., 2015; Wang et al., 2018; Zhang et al., 2017). As is well known, a high specific surface area for catalysts can supply more reaction sites and improve the adsorption capacity, but usually the specific surface area of metal oxides is very small. It

---

is generally agreed that the synthesis method and support may influence the catalytic activity of metal oxide catalysts. For example, some researchers have synthesized porous metal oxides with relatively high surface area by using porous silica as a template. In addition, transition metal oxides are also supported on oxides with high surface area such as mesoporous silica and aluminum oxides, and the interaction between active sites and the support is also an important factor in the improvement of catalytic activity. Therefore, the selection of a support is of great importance to improving the activity of catalysts. SBA-15 is one of the typical mesoporous silica materials and has been used widely in catalytic applications as a catalyst support due to its uniform mesoporous channels and high specific surface area (Li et al., 2017; Tang et al., 2017). Research on SBA-15 supported catalysts has been performed, and our group has investigated Mn/SBA-15 for toluene catalytic oxidation (Qu et al., 2013). In the previous study, the complete conversion temperature of toluene over Mn/SBA-15 catalysts prepared by the traditional wet impregnation method was more than 300°C, so there is still plenty of room for improvement. Modification of the supports is an effective method to improve the catalytic activity for supported catalysts. Adjusting the synthetic method or using additives is often used to achieve SBA-15 with different properties, such as pore structures and morphology. Different structures influence the adsorption properties and the dispersion of active sites, and pore size and pore structure may influence the formation of catalytically active species. In addition, the modification of the support may influence its interaction with active sites.

In the present work, SBA-15 mesoporous silica with three different morphologies and $MnO_x$ catalysts supported on the different types of SBA-15 were synthesized. The catalytic behavior in toluene oxidation was tested, and the properties of Mn/SBA-15 samples were investigated to confirm which factors are favorable to toluene catalytic oxidation.

# 1. Experimental

## 1.1. Materials and preparation

Three types of SBA-15 were synthesized as follows:

Rod-like SBA-15 was synthesized according to the report by Sayari et al. (2004). Triblock copolymer ($EO_{20}PO_{70}EO_{20}$, P123) (4.0 g) was dissolved in 120 mL 2 mol/L HCl aqueous solution under stirring for 4 hr, and then 8.5 g tetraethoxysilane (TEOS) was dissolved in the solution. The mixture was stirred at high-speed for 5 min and then aged for 20 hr. After being filtered and dried at 100°C for 24 hr, the product was calcined at 540°C for 10 hr. The sample is denoted as R-SBA-15.

Hexagonal SBA-15 was synthesized according to the report by Wang et al. (2011). P123 (4.0 g) was dissolved in 120 mL 2 mol/L HCl aqueous solution under stirring for 4 hr, and then 8.5 g TEOS was dissolved in the solution. $ZrOCl_2$ (4.66 g) was also dissolved in the aqueous solution. The mixture was stirred for 20 hr and aged in a Teflon reaction vessel at 100°C for 48 hr. Then the product was filtered, dried and calcined as in the synthesis of R-SBA-15 above. The sample is denoted as H-SBA-15.

Fiber-like SBA-15 was synthesized according to the report of Zhao et al. (1998). P123 (4.0 g) was dissolved in 120 mL 2 mol/L HCl aqueous solution under stirring, then 8.5 g TEOS was dissolved in the solution. The mixture was stirred for 4 hr and aged in a Teflon reaction container at 100°C for 48 hr. Then the product was collected by filtration, drying and calcining. The sample is denoted as F-SBA-15.

Mn/SBA-15 was synthesized by a precipitation method. Mn $(NO_3)_2$ aqueous solution and SBA-15 (R-SBA-15, H-SBA-15 or F-SBA-15) were added to a proper amount of deionized water while stirring. Then 1 mol/L $(NH_4)_2CO_3$ aqueous solution was added dropwise until the pH of the solution reached about 9. The mixture was aged at room temperature for 24 hr, and then the product was collected by filtration and drying. The three samples are denoted as Mn/R-SBA-15, Mn/H-SBA-15 and Mn/F-SBA-15, respectively.

## 1.2. Activity measurement

Toluene oxidation experiments were performed in a fixed-bed quartz microreactor with a continuous flow of 50 mL/min and the concentration was 500 ppm toluene +20%$O_2$/Ar balance. Mn/SBA-15 (0.2 g) catalyst was used in the experiment. The toluene conversion was analyzed when it reached steady state using an online gas chromatography (GC) with a flame ionization detector (GC-2014, Shimadzu, Japan).

## 1.3. Characterization

The characterization in the study was carried out as described in a previous report (Qin et al., 2017). Nitrogen adsorption–desorption isotherms were collected at 77 K (QUADRASORB-SI, Quantachrome, USA), and the specific surface areas were calculated with the Brunauer–Emmett–Teller (BET) equation. The pore volumes were determined at a relative pressure ($P/P_0$) value of 0.995, and the mean pore diameters were calculated with the Barrett–Joyner–Halenda (BJH) equation from the desorption branches of the isotherms. Scanning electron microscopy (SEM) was carried out on a scanning electron microscope (S-5500, Hitachi, Japan). Transmission electron microscopy (TEM) were carried out on a microscope with an operating voltage of 100 kV (Tecnai G2 Spirit, Thermo Fisher Scientific, USA). X-ray diffraction (XRD) patterns were collected using Cu $K\alpha$ radiation ($\lambda$ = 0.1542 nm) operating at 40 kV and 200 mA (D/max-$\gamma$b, Rigaku, USA). The patterns were carried out from 10° to 80° at a scan rate of 10°/min. $H_2$ temperature programmed reduction ($H_2$-TPR) measurements were carried out on a ChemBET with a thermal conductivity detector (TCD) (PULSAR, Quantachrome, USA). X-ray photoelectron spectroscopy (XPS) was carried out with an Al $K\alpha$ excitation source at a constant pass energy ($h\nu$ = 1486.6 eV) and all the results were adjusted with the binding energy of C1s (284.6 eV) (ESCALAB250, Thermo, USA).

# 2. Results and discussion

## 2.1. Activity for toluene catalytic oxidation

Fig. 1 shows the performance of toluene oxidation over different Mn/SBA-15 catalysts in the reaction temperature
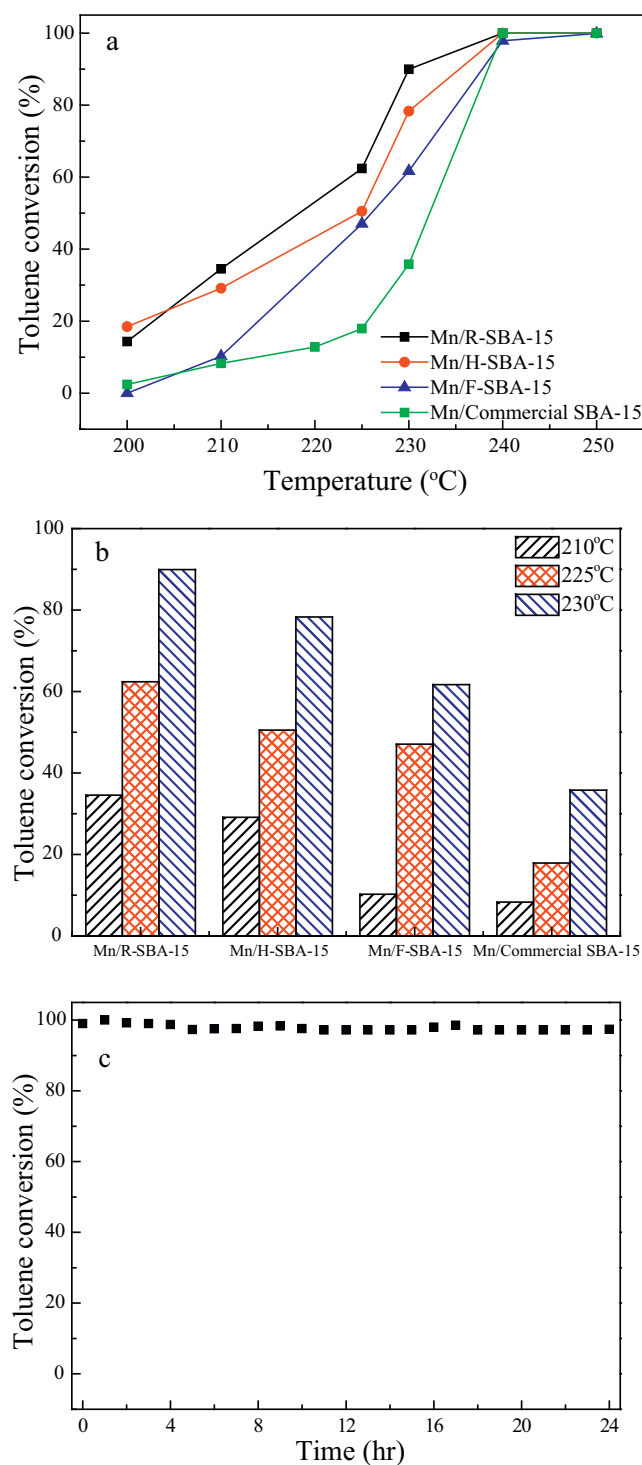
**Fig. 1 – (a) Toluene conversion performance over Mn based catalysts supported on different SBA-15 silicas, (b) toluene conversion at 210, 225 and 230°C, and (c) reaction stability of Mn/R-SBA-15. R-SBA-15, H-SBA-15 and F-SBA-15 refer to rod-like SBA-15, hexagonal SBA-15 and fiber-like SBA-15, respectively.**

ranges from 200 to 250°C. It is found that the rod-like SBA-15 supported $MnO_x$ catalyst exhibited better catalytic performance than the other as-synthesized Mn/SBA-15 catalysts.

When the temperature was increased to 230°C, the conversion of Mn/R-SBA-15 rose rapidly to 90%, whereas the other samples had not achieved conversion of 80%. The conversion of Mn/F-SBA-15 was only about 60% even though the temperature was 230°C. The catalytic ability of Mn/H-SBA-15 was between that of the other two catalysts. Therefore, it is quite clear that Mn/R-SBA-15 shows the best catalytic capacity, and the activity of three samples can be ranked as follows: Mn/R-SBA-15 > Mn/H-SBA-15 > Mn/F-SBA-15. Furthermore, the activity of Mn/commercial SBA-15 was compared with the three catalysts above. It is evident that the three catalysts have better activity than Mn/commercial SBA-15. In light of the results, it is believed that the difference of catalytic activity is highly related to the morphology and structure of the supports.

The reaction stability with time over the Mn/R-SBA-15 catalyst was tested at 240°C and the result is shown in Fig. 1c. The catalyst showed good reaction stability for toluene oxidation over a period of 24 hr, and the conversion remained above 95%. Herein, it is shown that the Mn/R-SBA-15 catalyst is a potential candidate catalyst for toluene combustion.

### 2.2. Morphology analysis of SBA-15 and diffusion of Mn/SBA-15

SEM images of three SBA-15 samples and TEM images of Mn/SBA-15 are shown in Fig. 2. The supports have different morphologies from each other. R-SBA-15 exhibits a morphology consisting of well-distributed short rods with length of 0.7–1.0 μm. The SEM image of H-SBA-15 displays particles of hexagonal shape and thickness of 0.625 μm. F-SBA-15 exhibits a morphology of long fiber type with the length of 20–30 μm. It can be observed from the TEM images that all three catalysts show well-ordered, uniform and hexagonal arrays of pore channels, which is a characteristic feature of SBA-15. Most $MnO_x$ is distributed outside the mesochannels due to the larger particle size. Distribution of $MnO_x$ on the catalysts is similar because the same synthesis method was used.

Nitrogen adsorption–desorption isotherms were measured to obtain textural information on the parent supports and Mn catalysts. As shown in Fig. 3, the isotherms for SBA-15 and Mn/SBA-15 samples are of type IV with a hysteresis loop of H1 type, which indicates that the parent mesoporous structure is well maintained during the synthesis process. The mesoporous channels are favorable for the diffusion of reactants. The BET results and pore structure parameters of all the samples are summarized in Table 1. The surface area of these three SBA-15 supports follows the order: H-SBA-15 > F-SBA-15 > R-SBA-15. After $MnO_x$ was supported on SBA-15, the surface area of the three catalysts declined to various extents, which means that $MnO_x$ is located on the outside of the support. The result is in agreement with the TEM results. Mn/R-SBA-15 has the lowest surface area. Generally, the surface area of the catalyst has a great effect on the catalytic capacity, as high surface area could result in high dispersion of metal or metal oxides and increase the chances of contacting reactants (Fu et al., 2016). However, from the activity and BET results it is found that the catalytic performance of the catalysts did not follow the order of surface area. This implies that the surface area is not a key factor in the performance of the as-synthesized Mn/SBA-15 catalysts in toluene oxidation.
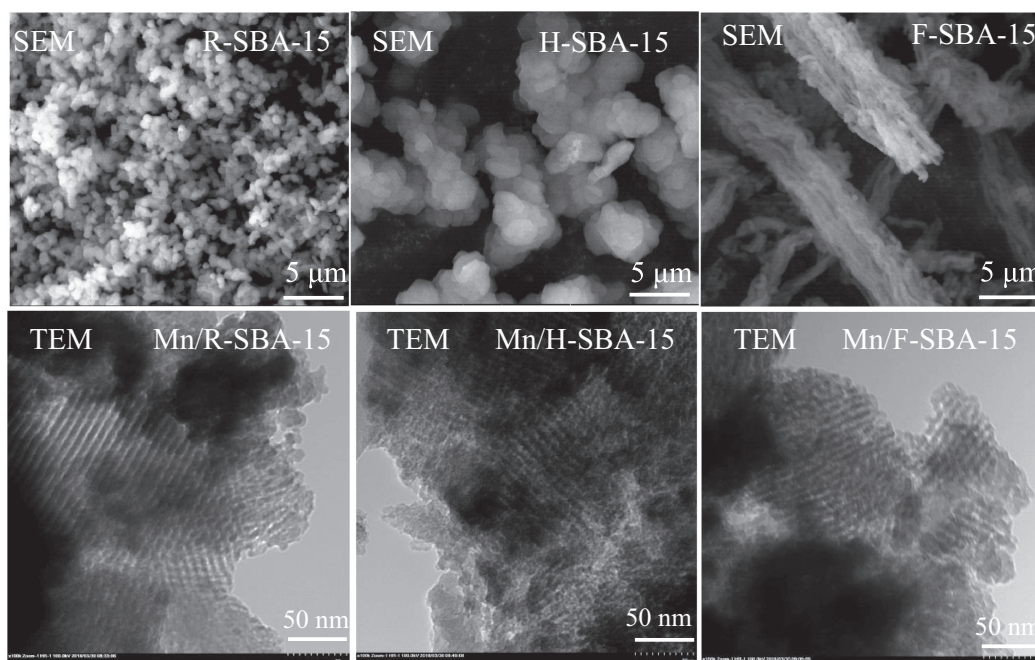
**Fig. 2 – Scanning electron microscopy (SEM) images of the three kinds of SBA-15 samples and transmission electron microscopy (TEM) images of the three Mn/SBA-15 catalysts.**

## 2.3. Confirmation of Mn species

XRD was used to further observe the structure of Mn species on the different supports, and the patterns are shown in Fig. 4. The big and broad diffraction peak at $2\theta = 22.4°$ is attributed to $SiO_2$, and the other peaks are attributed to manganese oxides. The peaks at $2\theta = 32.9°$ and $65.8°$ correspond to $Mn_2O_3$ (JCPDS 41–1442), and peaks at $2\theta = 36.6°$, $41.5°$ and $53.9°$ are attributed to $MnO_2$ (JCPDS 42–1316), indicating the coexistence of $Mn_2O_3$ and $MnO_2$ on the supports. It can be seen that the peaks of $Mn_2O_3$ become weaker gradually in the order Mn/R-SBA-15 > Mn/H-SBA-15 > Mn/F-SBA-15. The phenomenon suggests that the amount of $Mn_2O_3$ decreases in the same order as above or that the crystallinity of $Mn_2O_3$ on the catalysts decreases to gradually become amorphous.

## 2.4. Analysis of redox and chemical properties

The reducibility of $MnO_x$ on different SBA-15 supports was studied by $H_2$-TPR, and the profiles are presented in Fig. 5. These catalysts show two reduction peaks denoted as $\alpha$ and $\beta$. Generally, two reduction peaks occur for manganese oxides, denoting a two-step reductive process as follows: $Mn^{4+} \rightarrow Mn^{3+} \rightarrow Mn^{2+}$ (Huang et al., 2016; Wang et al., 2012). Specifically, the first peak corresponds to the reduction of $MnO_2/Mn_2O_3$ to $Mn_3O_4$, and the second one corresponds to the reduction of $Mn_3O_4$ to MnO (Dai et al., 2012; Zhang et al., 2015). It is worth noticing that the first peak can be deconvoluted into two peaks labeled as $\alpha_I$ and $\alpha_{II}$. According to previous reports, the peaks of $MnO_2$ can be assigned to the reduction of $MnO_2$ to $Mn_3O_4$ and $Mn_3O_4$ to MnO, respectively (Wang et al., 2009) and the peaks of $Mn_2O_3$ to the reduction of

$Mn_2O_3$ to $Mn_3O_4$ and $Mn_3O_4$ to MnO, respectively (Chen et al., 2014). According to the XRD results, we found that the $MnO_x$ consisted of $MnO_2$ and $Mn_2O_3$. Therefore, it is reasonable that peak $\alpha_I$ be assigned to the reduction of $MnO_2$ to $Mn_3O_4$ and peak $\alpha_{II}$ to the reduction of $Mn_2O_3$ to $Mn_3O_4$. The ratio of $\alpha_{II}/\alpha_I$ would then reflect the relationship of the amounts of $MnO_2$ and $Mn_2O_3$, and it is seen that the ratio of $\alpha_{II}/\alpha_I$ decreased in the order of Mn/R-SBA-15 > Mn/H-SBA-15 > Mn/F-SBA-15, indicating that Mn/R-SBA-15 possessed the most $Mn_2O_3$.

Comparing the reduction behavior of the samples, Mn/R-SBA-15 shows a lower reduction temperature than the other two, which indicates its better reducibility. The average valence and amount of $H_2$ consumption were calculated and listed in Table 1. From the table, the average valence of the samples increases in the order of Mn/R-SBA-15 < Mn/H-SBA-15 < Mn/F-SBA-15. The generally low average valence of Mn/R-SBA-15 suggests the existence of $Mn_2O_3$ or defect $Mn^{3+}$ generated in manganese oxides (Santos et al., 2010). For Mn/R-SBA-15, the low average valence is due to the high ratio of $\alpha_{II}/\alpha_I$, in other words, a large amount of $Mn_2O_3$. Usually, a higher amount of $H_2$ consumption represents more reducible oxygen species. In our study, the $H_2$ consumption of Mn/R-SBA-15 is 1.89 mmol/g, which is slightly smaller than that of Mn/H-SBA-15 (1.97 mmol/g). However, the tests of the catalytic activity of catalysts indicated that Mn/R-SBA-15 shows better catalytic activity than Mn/H-SBA-15, and the reduction temperature of Mn/H-SBA-15 is the highest. Thus, the oxygen mobility of the catalysts is more important for the oxidation of toluene when the difference in $H_2$ consumption is slight. Mn/F-SBA-15 has the lowest $H_2$ consumption of 1.67 mmol/g, and the oxygen mobility is lower than for the other two, so the activity is the poorest.
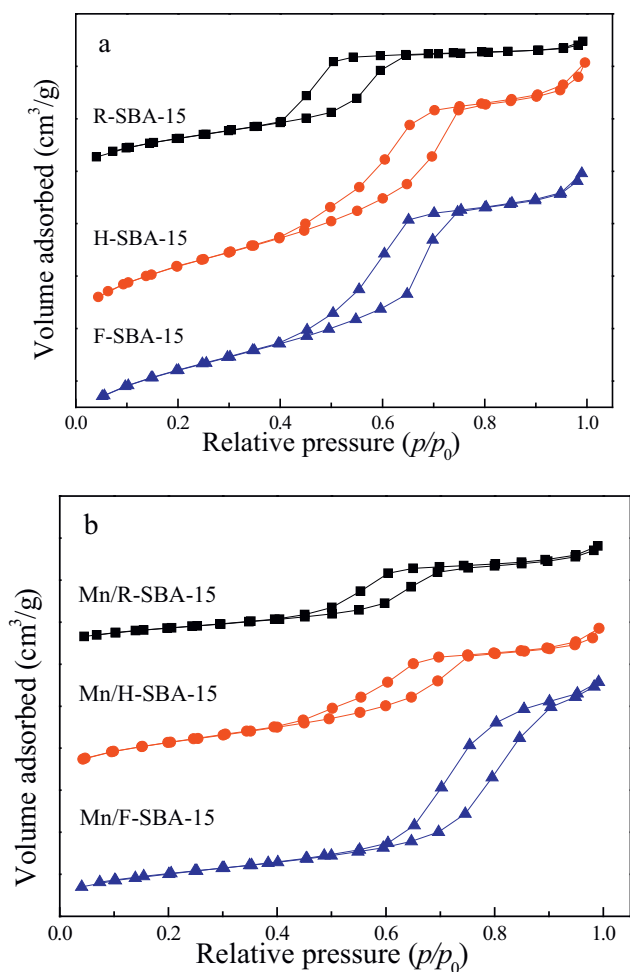
**Fig. 3 – N$_2$ adsorption/desorption isotherms of (a) parent SBA-15 samples and (b) catalysts.**
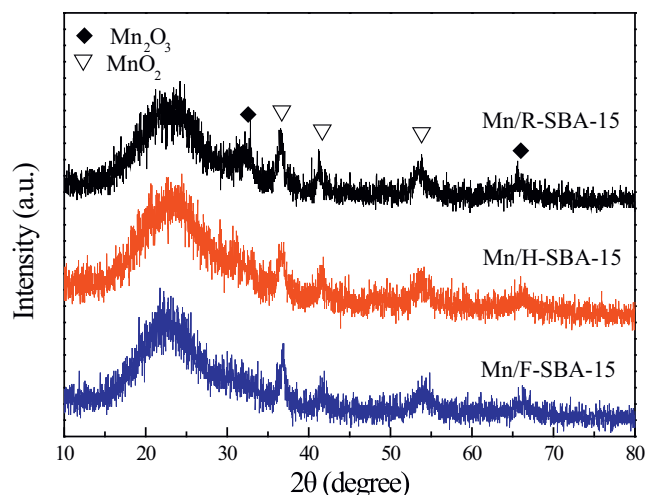


**Fig. 4 – X-ray diffraction (XRD) patterns of different Mn/SBA-15 catalysts.**

641.7 ± 0.2 eV). Similarly, the binding energies of O1s are also shifted to higher value than the theoretical values (529.5–529.9 and 531.2–531.5 eV) (Zhu et al., 2017). This high-energy shift from the theoretical value should be due to the interaction between MnO$_x$ and the silica support (Meng et al., 2013). The content of Mn$^{4+}$ on the surface of Mn/R-SBA-15 is 0.49, which is almost equal to that of Mn/H-SBA-15 and Mn/F-SBA-15 (0.47). The O1s spectra can be deconvoluted into two peaks attributed to surface lattice oxygen (O$_{latt}$, low binding energy) and surface adsorbed oxygen (O$_{ads}$, high binding energy). It can be seen from the table that the ratio of O$_{latt}$/O$_{ads}$ decreases in the order of Mn/R-SBA-15 (0.74) > Mn/H-SBA-15 (0.52) > Mn/F-SBA-15 (0.49). This result shows that Mn/R-SBA-15 contains the greatest amount of surface lattice oxygen.

## 2.5. Adsorption of toluene on Mn/SBA-15 catalysts

The catalytic capability of catalysts is determined not merely by the properties of the catalysts, but also their interaction with toluene, which is absolutely essential to investigate. Therefore, temperature programmed desorption (TPD) was performed to obtain information about the adsorption sites and interaction between the reactant and catalyst. Fig. 7 shows the toluene TPD profiles of Mn catalysts supported on different supports. The figure shows that only one desorption

XPS analysis was carried out, and the surface information for the samples is summarized in Table 2. Mn 2p$_{3/2}$ and O1s XPS spectra of the three samples are exhibited in Fig. 6. The asymmetric peaks of Mn 2p$_{3/2}$ spectra for all the catalysts can be deconvoluted into two peaks at binding energies of 643.9–644.4 and 642.0–642.1 eV, respectively. The components are attributed to surface Mn$^{4+}$ and Mn$^{3+}$ species, but the observed binding energies of Mn species are much higher than the theoretical values of Mn$^{4+}$ and Mn$^{3+}$ (643 ± 0.2 and

| Table 1 – Properties of SBA-15 and Mn/SBA-15 samples derived from the N$_2$ adsorption–desorption isotherms. | | | | | | |
|---|---|---|---|---|---|---|
| Sample | S$_{BET}$ (m$^2$/g) | V$_{total}$ (cm$^3$/g) | D$_{pore}$ (nm) | α$_{II}$/α$_{I}$ | AOS | H$_2$ consumption (mmol/g) |
| R-SBA-15 | 561.2 | 0.55 | 3.85 | | | |
| H-SBA-15 | 747.3 | 0.93 | 5.68 | | | |
| F-SBA-15 | 733.7 | 0.91 | 4.96 | | | |
| Mn/R-SBA-15 | 275.3 | 0.42 | 4.33 | 0.69 | 3.53 | 1.89 |
| Mn/H-SBA-15 | 504.9 | 0.64 | 5.65 | 0.49 | 3.57 | 1.97 |
| Mn/F-SBA-15 | 350.1 | 0.85 | 6.60 | 0.48 | 3.61 | 1.67 |

S$_{BET}$: specific surface area; V$_{total}$: primary total pore; D$_{pore}$: Barrett–Joyner–Halenda (BJH) mesopore diameter calculated from the desorption branch; α$_{II}$/α$_{I}$: ratio of two peaks deconvoluted from the first reduction peak; AOS: average oxidation state.
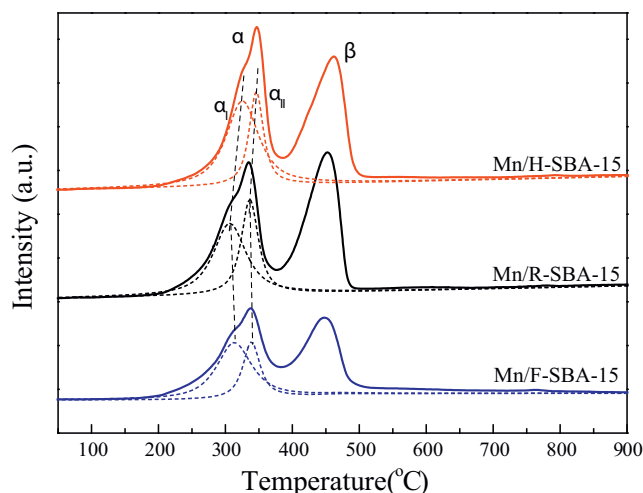
**Fig. 5 – H$_2$ temperature programmed reduction (H$_2$-TPR) of different Mn/SBA-15 catalysts.**

peak is present for each Mn/SBA-15 sample, and the temperatures of the peaks are in the range of 80–100°C. Mn/R-SBA-15 has the lowest desorption temperature, at 84°C, and the others are 100 and 91°C for Mn/H-SBA-15 and Mn/F-SBA-15, respectively. It is generally accepted that the desorption temperature is related to the reaction process, as a low desorption temperature means that it is easy for the reactant to desorb from inner pores and channels and diffuse onto the surface of the catalysts. That is to say, the diffusion of toluene molecules on Mn/R-SBA-15 is the best among the three, followed by Mn/F-SBA-15. The fact that Mn/R-SBA-15 had the best diffusion capability should be related to the morphology of R-SBA-15. The well-distributed short rods supply more mesochannel openings than the long fiber-like morphology of F-SBA-15, which is beneficial to the diffusion and adsorption of reactants (Kosuge et al., 2007). Therefore, the reaction takes place easily over Mn/R-SBA-15. Unexpectedly, Mn/H-SBA-15 shows the highest desorption temperature, but its activity is better than that of Mn/F-SBA-15. This is probably because the closely aggregated morphology of H-SBA-15 hinders the diffusion of toluene molecules, thereby increasing the desorption temperature. Nevertheless, other factors, such as abundant mobile oxygen species as observed from H$_2$-TPR results, may improve the activity of Mn/H-SBA-15.

### 2.6. Discussion

In view of the above results, one can see that Mn/SBA-15 catalysts display outstanding catalytic capability, and comparison of their
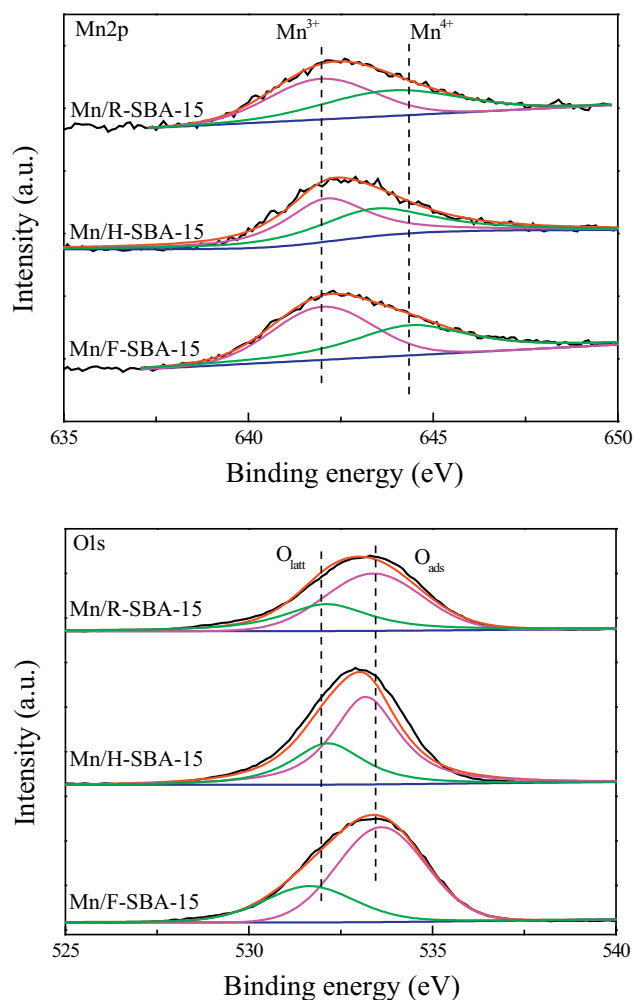


**Fig. 6 – X-ray photoelectron spectroscopy (XPS) spectra of different Mn/SBA-15 catalysts. O$_{ads}$: surface adsorbed oxygen; O$_{latt}$: surface lattice oxygen.**

performance with that of other catalysts in the literature is listed in Table 3. SBA-15 supports with different morphologies evidently affect the catalytic activity of Mn/SBA-15 catalysts. XRD shows that MnO$_2$ and Mn$_2$O$_3$ coexist on the supports. Nevertheless, a higher amount of Mn$_2$O$_3$ species was formed on the surface of MnO$_x$ supported on rod-like SBA-15. The peaks of Mn$_2$O$_3$ become weaker and weaker in the order Mn/R-SBA-15 > Mn/H-SBA-15 > Mn/F-SBA-15, which is in agreement with the order of catalytic activity. This suggests that the activity is affected by the properties of the manganese oxides. Combined with H$_2$-TPR results showing that the $\alpha_{II}/\alpha_I$ peak ratio is in agreement with

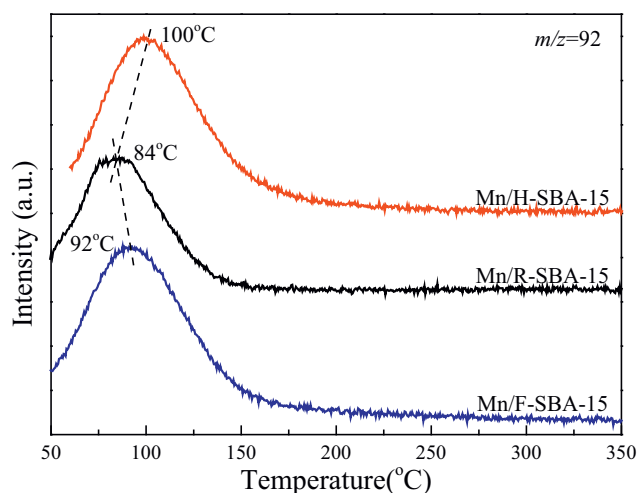| Table 2 – X-ray photoelectron spectroscopy results of the three Mn/SBA-15 catalysts. | | | | | | |
|---|---|---|---|---|---|---|
| Sample | Mn$^{4+}$ | Mn$^{3+}$ | Mn$^{4+}$/(Mn$^{3+}$+Mn$^{4+}$) | O$_{ads}$ | O$_{latt}$ | O$_{latt}$/O$_{ads}$ |
| Mn/R-SBA-15 | 644.4 eV | 642.0 eV | 0.49 | 533.4 eV | 532.1 eV | 0.74 |
| Mn/H-SBA-15 | 643.4 eV | 642.1 eV | 0.47 | 533.2 eV | 532.1 eV | 0.52 |
| Mn/F-SBA-15 | 643.9 eV | 642.0 eV | 0.47 | 533.6 eV | 531.7 eV | 0.49 |
| O$_{ads}$: surface adsorbed oxygen; O$_{latt}$: surface lattice oxygen. | | | | | | |

**Fig. 7 – Temperature programmed desorption of toluene over different Mn/SBA-15 catalysts. *m/z*: mass-to-charge ratio.**
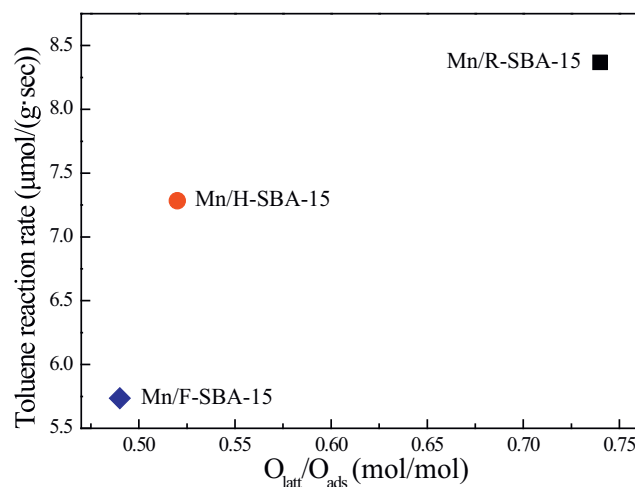


**Fig. 8 – Toluene consumption rates as a function of $O_{latt}/O_{ads}$ molar ratio of the three catalysts.**

XRD results, the highest amount of $Mn_2O_3$ is formed on Mn/R-SBA-15, followed by Mn/H-SBA-15. Taking into account the XPS results, the ratios of $Mn^{4+}$ and $Mn^{3+}$ on the catalysts are similar, but different $O_{latt}/O_{ads}$ ratios are observed, which vary in the order: Mn/R-SBA-15 > Mn/H-SBA-15 > Mn/F-SBA-15. Usually the ratio of $Mn^{3+}$ to $Mn^{4+}$ reflects the oxygen vacancies and surface oxygen species on a single oxide (Lin et al., 2016) and a previous study has clarified that a high $Mn^{3+}/Mn^{4+}$ implies a high $O_{ads}/O_{latt}$ ratio on $MnO_2$, based on the principle of electroneutrality (Wang et al., 2012). Therefore, considering the XRD and XPS results, this proves that surface $Mn^{3+}$ species do not come entirely from $MnO_2$ but also from $Mn_2O_3$ on the surface of the catalysts, and it is reasonable that $Mn_2O_3$ contributes to the surface lattice oxygen of the catalysts in addition to $MnO_2$. Our group's earlier study has proved that the existence of $Mn_2O_3$ improves the catalytic activity of the catalysts (Qu et al., 2013). Meanwhile, other researchers also reported that surface $Mn_2O_3$ species were favorable to the activity (Li et al., 2014). With respect to the activity and characterization results for the three catalysts, a conclusion can be reached that the lattice oxygen species play the major role in toluene catalytic oxidation. According to the Mars-van Krevelen (MVK) mechanism, lattice oxygen takes part in the reaction directly and is replenished by oxygen from the feed mixture. Additionally, the higher ratio of $O_{latt}/O_{ads}$ is directly related to the reaction rate (Fig. 8). Manganese oxides have great catalytic activity for VOC oxidation due to their strong oxygen storage/

release ability in the redox cycle taking place during the reaction process, and then high oxygen mobility effectively accelerates the catalytic activity. Among the three catalysts, Mn/R-SBA-15 has the best catalytic activity for toluene oxidation, and this is mainly due to the large amount of lattice oxygen from the mixed oxides of $Mn_2O_3$ and $MnO_2$ and having the highest oxygen mobility of the three catalysts, according to $H_2$-TPR results (Tang et al., 2014).

In general, inert supports are used to utilize their high specific surface area and diffusion of active components for the improvement of activity. Nevertheless, in this study the activity is not simply associated with the specific surface area. Mn/F-SBA-15, with high specific surface area (733.7 $m^2/g$), has the lowest activity in toluene oxidation among the studied catalysts. Therefore, the properties of manganese oxides on the supports directly affect the catalytic activity of the catalysts. SBA-15 with rod-like morphology has the most positive effect on the properties of manganese oxides compared to the other two morphologies. This is probably because the structure of R-SBA-15 is favorable for the formation of $Mn_2O_3$. Recently, some researchers have pointed out that SBA-15 microporosity should be more appropriately be described as surface roughness, and the roughness directly impacts the formation of $VO_x$ on SBA-15 (Smith et al., 2014). Therefore, it is believed that the properties of SBA-15 lead to formation of different manganese oxides, and in our study the morphology of SBA-15 clearly has a great influence on the properties of manganese oxides, such as crystallinity and redox ability. It was also discovered that the capability of desorption is different for the three catalysts, and the difference is probably caused by the pore structures of the catalysts. In summary, Mn/R-SBA-15, with a large amount of lattice oxygen and high mobility, is an excellent catalyst for toluene catalytic oxidation, and rod-like SBA-15 is beneficial to the catalytic activity.

**Table 3 – Catalytic activity of toluene oxidation reported in the literature.**

| Catalysts | $T_{98\%}$ | Reference |
|---|---|---|
| $Mn_2O_3$ | 325°C | Sihaib et al., 2017 |
| $MnO_x$/HZSM-5 | 270°C | Zhang et al., 2018 |
| Cu0.5Mn0.75/$Al_2O_3$ | 325°C | Wang et al., 2017 |
| Mn0.5/$Al_2O_3$ | 450°C | |
| Mn14.1–400 | 275°C | Liu et al., 2017 |
| Mn/R-SBA-15 | 240°C | This work |

$T_{98\%}$: temperature when the conversion is 98%.

## 3. Conclusions

This study revealed that SBA-15 with different morphologies and structures greatly affected the catalytic activity of Mn/

SBA-15 for toluene oxidation. Mn/R-SBA-15 showed the best catalytic activity among the three, and the conversion at 230°C was about 15% and 30% higher than that of Mn/H-SBA-15 and Mn/F-SBA-15, respectively. Firstly, the diffusion of toluene on Mn/R-SBA-15 was the fastest and the catalytic reaction had the highest rate. Secondly, the R-SBA-15 support evidently influences the formation of $MnO_x$, and more $Mn_2O_3$ is formed on Mn/R-SBA-15 than on the other supports. The mixed oxides of $Mn_2O_3$ and $MnO_2$ on R-SBA-15 supply more lattice oxygen species, which is favorable for the activity according to the MVK mechanism. Thirdly, the high oxygen mobility of Mn/R-SBA-15 accelerates the activity. Therefore, the excellent activity of Mn/R-SBA-15 contributes to the formation of more surface $Mn_2O_3$ species, lattice oxygen species and high oxygen mobility.

## Acknowledgments

## REFERENCES

Chen, H.H., Zhang, H.P., Yan, Y., 2014. Fabrication of porous copper/manganese binary oxides modified ZSM-5 membrane catalyst and potential application in the removal of VOCs. Chem. Eng. J. 254, 133–142.

Dai, Y., Wang, X.Y., Dai, Q.G., Li, D., 2012. Effect of Ce and La on the structure and activity of $MnO_x$ catalyst in catalytic combustion of chlorobenzene. Appl. Catal. B Environ. 111-112, 141–149.

Du, J.P., Qu, Z.P., Dong, C., Song, L.X., Qin, Y., Huang, N., 2018. Low-temperature abatement of toluene over Mn-Ce oxides catalysts synthesized by a modified hydrothermal approach. Appl. Surf. Sci. 433, 1025–1035.

Fu, X.R., Liu, Y., Yao, W.Y., Wu, Z.B., 2016. One-step synthesis of bimetallic Pt-Pd/MCM-41 mesoporous materials with superior catalytic performance for toluene oxidation. Catal. Commun. 83, 22–26.

Guo, Y.Y., Zhang, S., Zhu, J., Su, L.Q., Xie, X.M., Li, Z., 2017. Effects of Pt on physicochemical properties over Pd based catalysts for methanol total oxidation. Appl. Surf. Sci. 416, 358–364.

He, C., Zhang, F.W., Yue, L., Shang, X.S., Chen, J.S., Hao, Z.P., 2012. Nanometric palladium confined in mesoporous silica as efficient catalysts for toluene oxidation at low temperature. Appl. Catal. B Environ. 111, 46–57.

Huang, H., Zhang, C.H., Wang, L., Li, G.Q., Song, L., Li, G.C., et al., 2016. Promotional effect of HZSM-5 on the catalytic oxidation of toluene over $MnO_x$/HZSM-5 catalysts. Catal. Sci. Technol. 6, 4260–4270.

Kosuge, K., Kubo, S., Kikukawa, N., Takemori, M., 2007. Effect of pore structure in mesoporous silicas on VOC dynamic adsorption/desorption performance. Langmuir 23, 3095–3102.

Li, J.J., Li, L., Cheng, W., Wu, F., Lu, X.F., Li, Z.P., 2014. Controlled synthesis of diverse manganese oxide-based catalysts for complete oxidation of toluene and carbon monoxide. Chem. Eng. J. 244, 59–67.

Li, X.X., Guo, L.L., He, P.C., Yuan, X., Jiao, F.P., 2017. Co-SBA-15-immobilized NDHPI as a new composite catalyst for toluene aerobic oxidation. Catal. Lett. 147, 856–864.

Liao, Y.N., He, L.F., Man, C.G., Chen, L.M., Fu, M.L., Wu, J.L., et al., 2014. Diameter-dependent catalytic activity of ceria nanorods with various aspect ratios for toluene oxidation. Chem. Eng. J. 256, 439–447.

Lin, T., Yu, L., Sun, M., Cheng, G., Lan, B., Fu, Z.W., 2016. Mesoporous $\alpha$-$MnO_2$ microspheres with high specific surface area: controlled synthesis and catalytic activities. Chem. Eng. J. 286, 114–121.

Liu, P., He, H.P., Wei, G.L., Liu, D., Liang, X.L., Chen, T.H., et al., 2017. An efficient catalyst of manganese supported on diatomite for toluene oxidation: manganese species, catalytic performance, and structure-activity relationship. Microporous Mesoporous Mater. 239, 101–110.

Lu, H.F., Kong, X.X., Huang, H.F., Zhou, Y., Chen, Y.F., 2015. Cu–Mn–Ce ternary mixed-oxide catalysts for catalytic combustion of toluene. J. Environ. Sci. 32, 102–107.

Meng, Y.T., Genuino, H.C., Kuo, C.H., Huang, H., Chen, S.Y., Zhang, L.C., et al., 2013. One-step hydrothermal synthesis of manganese-containing MFI-type zeolite, Mn-ZSM-5, characterization, and catalytic oxidation of hydrocarbons. J. Am. Chem. Soc. 135, 8594–8605.

Qin, Y., Qu, Z.P., Dong, C., Huang, N., 2017. Effect of pretreatment conditions on catalytic activity of Ag/SBA-15 catalyst for toluene oxidation. Chin. J. Catal. 38, 1603–1612.

Qu, Z.P., Bu, Y.B., Qin, Y., Wang, Y., Fu, Q., 2013. The improved reactivity of manganese catalysts by Ag in catalytic oxidation of toluene. Appl. Catal. B Environ. 132-133, 353–362.

Santos, V.P., Pereira, M.F.R., Órfão, J.J.M., Figueiredo, J.L., 2010. The role of lattice oxygen on the activity of manganese oxides towards the oxidation of volatile organic compounds. Appl. Catal. B Environ. 99, 353–363.

Sayari, A., Han, B.H., Yang, Y., 2004. Simple synthesis route to monodispersed SBA-15 silica rods. J. Am. Chem. Soc. 126, 14348–14349.

Sihaib, Z., Puleo, F., Garcia-Vargas, J.M., Retailleau, L., Descorme, C., Liotta, L.F., et al., 2017. Manganese oxide-based catalysts for toluene oxidation. Appl. Catal. B Environ. 209, 689–700.

Smith, M.A., Zoelle, A., Yang, Y., Rioux, R.M., Hamilton, N.G., Amakawa, K., et al., 2014. Surface roughness effects in the catalytic behavior of vanadia supported on SBA-15. J. Catal. 312, 170–178.

Tang, W.X., Wu, X.F., Li, D.Y., Wang, Z., Liu, G., Liu, H.D., et al., 2014. Oxalate route for promoting activity of manganese oxide catalysts in total VOCs' oxidation: effect of calcination temperature and preparation method. J. Mater. Chem. A 2, 2544–2554.

Tang, W.X., Deng, Y.Z., Chen, Y.F., 2017. Promoting effect of acid treatment on Pd-Ni/SBA-15 catalyst for complete oxidation of gaseous benzene. Catal. Commun. 89, 86–90.

Wang, L.C., Liu, Q., Huang, X.S., Liu, Y.M., Cao, Y., Fan, K.N., 2009. Gold nanoparticles supported on manganese oxides for low-temperature CO oxidation. Appl. Catal. B Environ. 88, 204–212.

Wang, F., Li, J.S., Yuan, J.F., Sun, X.Y., Shen, J.Y., Han, W.Q., et al., 2011. Short channeled Zr-Ce-SBA-15 supported palladium catalysts for toluene catalytic oxidation. Catal. Commun. 12, 1415–1419.

Wang, F., Dai, H.X., Deng, J.G., Bai, G.M., Ji, K.M., Liu, Y.X., 2012. Manganese oxides with rod-, wire-, tube-, and flower-like morphologies: highly effective catalysts for the removal of toluene. Environ. Sci. Technol. 46, 4034–4041.

Wang, H.P., Lu, Y.Y., Han, Y.X., Lu, C.L., Wan, H.Q., Xu, Z.Y., et al., 2017. Enhanced catalytic toluene oxidation by interaction between copper oxide and manganese oxide in Cu-O-Mn/$\gamma$-$Al_2O_3$ catalysts. Appl. Surf. Sci. 420, 260–266.

Wang, C., Yu, F., Zhu, M.Y., Tang, C.J., Zhang, K., Zhao, D., et al., 2018. Highly selective catalytic reduction of NOx by $MnO_x$-$CeO_2$–$Al_2O_3$ catalysts prepared by self-propagating

high-temperature synthesis. J. Environ. Sci. https://doi.org/
  10.1016/j.jes.2018.03.011.

Yang, H.G., Deng, J.G., Liu, Y.X., Xie, S.H., Wu, Z.X., Dai, H.X., 2016.
  Preparation and catalytic performance of Ag, Au, Pd or Pt
  nanoparticles supported on 3DOM $CeO_2$ -$Al_2O_3$ for toluene
  oxidation. J. Mol. Catal. A Chem. 414, 9–18.

Zhang, J., Zhang, C., He, H., 2015. Remarkable promotion effect of
  trace sulfation on OMS-2 nanorod catalysts for the catalytic
  combustion of ethanol. J. Environ. Sci. 35, 69–75.

Zhang, X.D., Li, H.X., Hou, F.L., Yang, Y., Dong, H., Liu, N., et al.,
  2017. Synthesis of highly efficient $Mn_2O_3$ catalysts for CO
  oxidation derived from Mn-MIL-100. Appl. Surf. Sci. 411, 27–33.

Zhang, C., Huang, H., Li, G., Wang, L., Song, L., Li, X., 2018. Zeolitic
  acidity as a promoter for the catalytic oxidation of toluene over

$MnO_x$/HZSM-5 catalysts. Catal. Today https://doi.org/10.1016/j.
  cattod.2018.03.019.

Zhao, D.Y., Feng, J.L., Huo, Q.S., Melosh, N., Fredrickson, G.H.,
  Chmelka, B.F., et al., 1998. Triblock copolymer syntheses of
  mesoporous silica with periodic 50 to 300 Angstrom pores.
  Science 279, 548–552.

Zhu, X.C., Zhang, S., Yu, X.N., Zhu, X.B., Zheng, C.H., Gao, X., et al.,
  2017. Controllable synthesis of hierarchical $MnO_x$/$TiO_2$
  composite nanofibers for complete oxidation of
  low-concentration acetone. J. Hazard. Mater. 337, 105–114.